

# Gaussian decomposition of H I surveys

## V. Search for very cold clouds

U. Haud

Tartu Observatory, 61 602 Tõravere, Tartumaa, Estonia  
e-mail: urmas@aaai.ee

Received 25 September 2009 / Accepted 20 January 2010

### ABSTRACT

**Context.** In the previous papers of this series, we decomposed all the H I 21-cm line profiles of the Leiden-Argentina-Bonn (LAB) database into Gaussian components (GCs), and studied the statistical distributions of the obtained GCs.

**Aims.** Now we are interested in separating the “clouds” of similar closely spaced GCs from the general database of the components. In this paper we examine the most complicated case for our new cloud-finding algorithm – the clouds of very narrow GCs.

**Methods.** To separate the clouds of similar GCs, we started with the single-link hierarchical clustering procedure in five-dimensional (longitude, latitude, velocity, GC width, and height) space, but made some modifications to accommodate it to the large number of components. We also used the requirement that each cloud may be represented at any observed sky position by only one GC and take the similarity of global properties of the merging clouds into account. We demonstrate that the proposed algorithm enables us to find the features in gas distribution, which are described by similar GCs. As a test, we applied the algorithm for finding the clouds of the narrowest H I 21-cm line components.

**Results.** Using the full sky search for cold clouds, we easily detected the coldest known H I clouds and demonstrate that actually they are a part of a long narrow ribbon of cold clouds. We modeled these clouds as a part of a planar gas ring, then deduce their spatial placement and discuss their relation to supernova shells in the solar neighborhood. Many other narrow-lined H I structures are also found. We conclude that the proposed algorithm satisfactorily solves the posed task. In testing the algorithm, we found a long ribbon of very cold H I clouds and demonstrated that all the observed properties of this band of clouds are described very well by the planar ring model.

**Conclusions.** We also guess that the study of the narrowest H I 21-cm line components may be a useful tool for finding the structure of neutral gas in solar neighborhood.

**Key words.** ISM: atoms – ISM: clouds – radio lines: ISM

## 1. Introduction

In earlier papers of this series, we described the Gaussian decomposition of large H I 21-cm line surveys (Haud 2000, hereafter Paper I) and the use of the obtained GCs for detecting of different observational and reductional problems (Haud & Kalberla 2006, hereafter Paper II), for separating thermal phases in the interstellar medium (ISM; Haud & Kalberla 2007, hereafter Paper III) and for studying intermediate and high-velocity hydrogen clouds (IVCs and HVCs; Haud 2008, hereafter Paper IV). A detailed justification for the use of Gaussian decomposition in these studies was provided in Paper III. Observational data for the decomposition came from the LAB database of H I 21 cm line profiles, which combines the new revision (LDS2, Kalberla et al. 2005) of the Leiden/Dwingeloo Survey (LDS, Hartmann 1994) and a similar Southern sky survey (IARS, Bajaja et al. 2005) completed at the Instituto Argentino de Radioastronomia. The LAB database is described in detail by Kalberla et al. (2005). Our method of Gaussian decomposition generated 1 064 808 GCs for 138 830 profiles from LDS2 and 444 573 GCs for 50 980 profiles from IARS.

In Papers II–IV, we used each obtained GC as a single entity, which is independent of all other GCs, and analyzed statistical distributions of their parameters. These results indicated that different structures in the ISM could be recognized as density

enhancements in the distribution of GC parameters in the five-dimensional parameter space or that the well-defined GCs with similar parameters at least statistically define the related objects, which share the same physical state in real space. The situation may be more complicated in the cases of heavily blended GCs in emission lines near the galactic plane. These earlier papers also demonstrate the importance of the GC widths, the knowledge of which helps us separate the components, corresponding to different physical structures of the ISM or to the artifacts of the observations, reduction, and the Gaussian decomposition itself. The third point, which is clear from the earlier studies, is that in reality many H I structures, observable in sky, extend to much larger areas than covered by a single beam of the radio telescope. This means that some GCs of the neighboring profiles may represent the features of a similar origin and that they are not independent of the others, so may be grouped together to represent larger structures.

In the present paper, we start studying these similarities and relations between the GCs, by defining clouds of similar GCs, which may (but need not) describe the real gas concentrations in the real space. In doing so, we must keep in mind that there are no precise definitions of the terms such as “cloud”, “clump”, or “core” (Larson 2003), and the physical reality of the clumps, found by different authors, has been a matter of controversial

debate since the presentation of the first systematic attempts to identify any kind of gas clumps. Nevertheless, many papers have been devoted to the study of clouds, clumps, and cores in the ISM.

As the structure in molecular clouds determines, in part, the locations, numbers, and masses of newly formed stars, much effort has been invested in characterizing this gas. The clumpy substructure of molecular clouds was first identified by eye (Blitz & Stark 1986; Carr 1987; Loren 1989; Nozawa et al. 1991; Lada et al. 1991; Blitz 1993; Dobashi et al. 1996). However, as a power-law mass spectrum predicts an increasing number of smaller and smaller clumps, confusion is usually the limiting factor in clump identification by eye. It is thus highly desirable to use automated clump-finding algorithms in the analysis of observed data, as the use of an algorithm allows the structure to be analyzed in a consistent and stable way (Kramer et al. 1998).

The two applications that have the most shaped molecular line astronomy are the clump identification algorithms GAUSSCLUMP by Stutzki & Güsten (1990) and CLUMPFIND by Williams et al. (1994). GAUSSCLUMPS uses a least square fitting procedure to decompose the emission iteratively into one or more Gaussian clumps. CLUMPFIND associates each local emission peak and the neighboring pixels with one clump (similar to the usual eye inspection procedure). Although the basic concept of both algorithms is quite different, they give consistent results for the larger clumps, when used on the same data (Williams et al. 1994). With H I data Thilker (1998) has used an algorithm, somewhat similar to GAUSSCLUMPS, and applied it to look for H I bubbles blown by supernovas in external galaxies. The method, similar to CLUMPFIND, was used by de Heij et al. 2002 to automatically search for compact high velocity clouds (HVCs) in the Leiden/Dwingeloo Survey.

Later Nidever et al. (2008) have used the Gaussian decomposition of the LAB profiles with the algorithm created according to the description of our decomposition program in Paper I. The obtained GCs are then used to disentangle overlapping H I structures. They stress that using GCs makes it possible to distinguish different H I filaments even when they are overlapping in velocity. They state that in these situations the GCs trace structures that are real, and they may even contain physical information about the structures. They were successful in tracking tenuous structures through rather complicated environments, even though the decomposition of those environments likely carries no physical meaning. The results were used to study the origin of the Magellanic Stream and its leading arm.

We would like to move a step further and use an automatic computer program for finding different continuous H I features in the full decomposition of the LAB database. In the next section, we give a brief description of the algorithm for finding coherent structures in the large database of GCs. The details of our algorithm are published in [arXiv:1001.4155v1]. Here we argue that the most complicated case for our cloud-finding approach are the clouds of the narrowest GCs, and concentrate our attention on the test with such cold clouds. Therefore, as the first step we have applied the program for the full sky search of the coldest H I clouds in the Galaxy, which could be identified using the LAB data. Then we argue that this search has rediscovered some of the coldest clouds observed so far in H I emission, and demonstrate that these known clouds actually constitute only a small part of a considerably larger coherent structure. Finally, we describe this structure with the help of a planar ring model, deduce its location in the space, and discuss the possible relations with some supernova shells in the Local Bubble (LB).

However, during all these studies we must keep in mind that the widths of such narrow GCs, as used in this paper, most likely are not correct representations of the actual widths of the underlying H I 21-cm emission lines. Because of both the finite optical depth of the lines and the velocity resolution of the LAB survey, the GC widths used here are mostly the upper limits for the actual line widths. Therefore, they cannot be used to the study physical properties in the clouds, but as the actual lines are even narrower than the corresponding GCs, we may still state that we are looking for very narrow lines and very cold gas clouds.

## 2. The cloud-finding algorithm

The task of finding the clouds of similar objects belongs to cluster analysis. As in previous papers of this series, we have studied some distributions of GCs, considering all components more or less independent of each other, so it is now natural to follow some agglomerative (bottom-up) hierarchical clustering procedure. If we are looking for clouds whose parameters vary smoothly from one point to another, the most appropriate algorithm seems to be single-link clustering. We add to the existing cluster a new element, which is the closest to at least one of the elements of this cluster. However, we faced some problems with direct use of the single-link clustering.

In the Galaxy, H I has a rather complicated spatial and kinematic structure, so that the Gaussian decompositions of the profiles, particularly near the galactic plane, may be rather complicated and contain many different GCs per profile. Running the preliminary versions of our cluster identification program demonstrated that, without applying special restrictions, one dominating cloud started to emerge around the galactic plane from the first steps of the merging process. Finally only these H I structures were distinguishable, whose properties differ very strongly from those of general ISM. We would instead like to achieve opposite results: to separate all the pieces of more or less coherent structures and follow them as close as possible to other structures, but not to merge probably different features. To achieve this, we decided that every GC of the profile must represent a different feature of the gas in a particular sky position.

For example, in HVCs we often get two GCs in the same profile at nearly the same velocity, and most likely they both describe the same physical cloud, but the narrow GC represents the properties of the gas in compact cold cores, and the wider component describes the gas in the more extended warmer envelope of the cloud (Kalberla & Haud 2006; Paper IV). We decided to consider such features as different entities of ISM and therefore to apply a restriction that every cloud of GCs may only contain one component from each profile. In this way, if in some problems we need to consider “cores” and “envelopes” together, we may join corresponding clouds for this particular task, but if we allow them to merge from the beginning, it would be harder to separate out different subclouds for some other studies.

One more problem emerged at later stages of the merging of GCs into clouds. By using a pure single-link clustering algorithm, we sometimes found the cases where two clouds with rather different average properties merged, as they touched each other at some point on their outer perimeter. As this was undesirable, we added a test of the similarity of global properties of the merging subclouds, and actually merged them only in those cases where this similarity was above a predefined limit.

Besides the algorithm of joining different GCs into clouds, an important step in any cluster-finding process is also the selection of a distance measure, which will determine how the similarity of two elements is calculated. After testing some

possibilities, we decided to quantify the dissimilarity of the GCs  $E_i$  and  $E_j$  of neighboring profiles with the parameter

$$S' = \frac{\int_{-\infty}^{\infty} (E_i - E_j)^2 dV}{\int_{-\infty}^{\infty} E_i^2 dV + \int_{-\infty}^{\infty} E_j^2 dV}, \quad (1)$$

where the GCs  $E$  are given by

$$E(x) = T \exp \left[ -\frac{(x - V)^2}{2W^2} \right], \quad (2)$$

and  $T$  is the height of the component at its central velocity  $V$ , and  $W$  determines the width of the GC. Integrating and for computational convenience applying the transformation  $S = -\ln(1 - S')$ , we get

$$S = \frac{(V_i - V_j)^2}{2(W_i^2 + W_j^2)} - \ln \left[ 2 \frac{T_i W_i T_j W_j}{T_i^2 W_i + T_j^2 W_j} \left( \frac{2}{W_i^2 + W_j^2} \right)^{1/2} \right]. \quad (3)$$

The parameter  $S$ , as defined by Eq. (3), compares the values of two Gaussian functions at all possible velocities and corresponds to the natural human understanding of the similarity of two curves: they are similar when they are close to each other everywhere. The parameter  $S = 0$ , when two GCs have exactly the same values of their parameters and for increasingly different components  $S \rightarrow \infty$ .

It is easy to see that this definition also compensates for uncertainties in the determination of the GC parameters, as discussed in Sect. 4.2. of the Paper I. For example, in the presence of noise our decomposition program gives the most unreliable values for the central velocities and widths for the widest GCs (component D in Fig. 10 of Paper I). However, when the line widths become larger, the differences in central velocities and also in widths become less important in the first addend of Eq. (3). Therefore, we may conclude that our dissimilarity measure treats the observed lines of different width with more or less the same precision. This is good for comparing two independent GCs, but may pose problems for the clustering, because all natural gradients in parameter values become increasingly important for narrower components. It may make the detection of small, bright, but cold clouds of HI rather problematic. Therefore, we decided to test our approach with the narrowest GCs found in the decomposition of the LAB.

### 3. Search for very cold clouds

To our knowledge, the coldest clouds in the Galaxy, found so far in HI emission, are the two gas concentrations at near-zero velocity around ( $l = 225^\circ, b = +44^\circ$ ) and ( $l = 236^\circ, b = +45^\circ$ ), discovered by Verschuur (1969) and afterwards studied in more details by Verschuur & Knapp (1971) and Knapp & Verschuur (1972). Later, the third cloud around ( $l = 213^\circ, b = +41^\circ$ ) was added to the first two by Heils & Troland (2003), and one of the recent detailed studies of these clouds is the one by Meyer et al. (2006). They observed the interstellar Na I D1 and D2 absorption toward 33 stars, derived a cloud temperature of  $20^{+6}_{-8}$  K, and placed a firm upper limit of 45 pc on the distance of the clouds. This distance corresponds to the upper limit of the linear size of the clouds of about 5 pc. Redfield & Linsky (2008) interpret these clouds as the result of the collision of the warm high-velocity Gem Cloud with the slower moving Leo, Aur, and LIC clouds in the Local Interstellar Medium (LISM). At the same time, the properties of the clouds also seem to be similar to the temperatures (mostly  $10 < T_S < 40$  K) and to dimensions (in

parsec scale) of numerous HI self-absorption features, found near the galactic plane (e.g. Gibson et al. 2000; Dickey et al. 2003; Kavars 2005; Hosokawa & Inutsuka 2007). Our interest in the subject is to test whether the clustering algorithm finds these clouds.

For this test we first constructed the dendrogram for all GCs in our decomposition and inspected the resulting clouds for different values of the cutting level of the dendrogram. From this inspection, we chose the value  $S_{Cu} = 0.44$  for the final cutting level. In this way we obtained 94 874 clusters of GCs, and 236 306 components remained detached from the others. The largest cloud (12 585 GCs) in the obtained list corresponds to a relatively smooth warm neutral medium at high galactic latitudes, but the list also contains many very small clouds of 2–3 GCs each (the cluster size distribution follows the power law with a slope of about 1.9). As Verschuur & Knapp (1971) have estimated that their cool clouds have diameters of at least  $1.5^\circ$ , we are not interested in the smallest clouds in our list, and in the following, we only consider the clouds that contain at least 7 GCs (in LAB one profile represents an area of 0.25 square degrees and 7 profiles cover the area, corresponding to the cloud with the diameter of  $1.5^\circ$ ). In our list, there are 21 224 clouds of this size.

To search for the coldest clouds in the list, we must apply some additional selection criteria. First of all, we are looking for clouds that consist of relatively narrow GCs. In Paper III, we demonstrated that the mean line-width of the HI 21-cm radio lines of the cold neutral medium of our Galaxy is  $FWHM = 3.9 \pm 0.6$  km s $^{-1}$ . Therefore, the gas, with  $FWHM \leq 3.0$  km s $^{-1}$ , may already be considered as a very cold gas, so we look for the clouds where the mean width of the GCs is below this limit. In Paper II, we also demonstrated that many weak and/or very narrow GCs do not represent the actual HI emission of the Galaxy, but are more likely caused by observational noise or radio interferences. Here we are not interested in these GCs, so we apply the selection criteria, given by Eqs. (4) and (5) of Paper II. However, now we do not apply these criteria to single GCs, but to the clouds obtained from our clustering process.

From Eqs. (4) and (5) of Paper II, it follows that the narrowest GCs, which most likely represent the galactic HI, have the heights  $\gtrsim 0.95$  K. Therefore, we consider only those clouds for which the mean height of their GCs is  $\geq 1.0$  K. At first sight, a similar selection ( $FWHM \geq 1.25$  km s $^{-1}$ , corresponding to Eq. (4) of Paper II) may also be applied to the width of the GCs. However, we are looking for clouds with the narrowest GCs, and some of the real lines may be even narrower than interferences with  $T \geq 1.0$  K. Therefore, as this selection may reject not only the interferences, but also a considerable amount of GCs that are the main interest in our study, this selection cannot be applied directly. At the same time, the selection rule given by Eq. (4) of Paper II applies only statistically, and it turned out that better results can be obtained by rejecting the clouds, for which more than half of their GCs do not satisfy Eq. (4) of Paper II. Nevertheless, some confusion with the interferences still remains.

After applying all the described selection criteria, we had a list of 1 380 cold clouds. However, when looking at these clouds, we saw that the clouds with the highest velocities (concentrated around  $+50$  and  $+100$  km s $^{-1}$ ) were only located in a very narrow band around the galactic plane (all at  $|b| < 22^\circ$ , most at  $|b| < 5^\circ$ ). We have stressed several times that the Gaussian decomposition gives relatively unreliable results in these regions, and the corresponding GCs are probably not directly related to the physical properties of the ISM. Therefore, we decided to also reject those

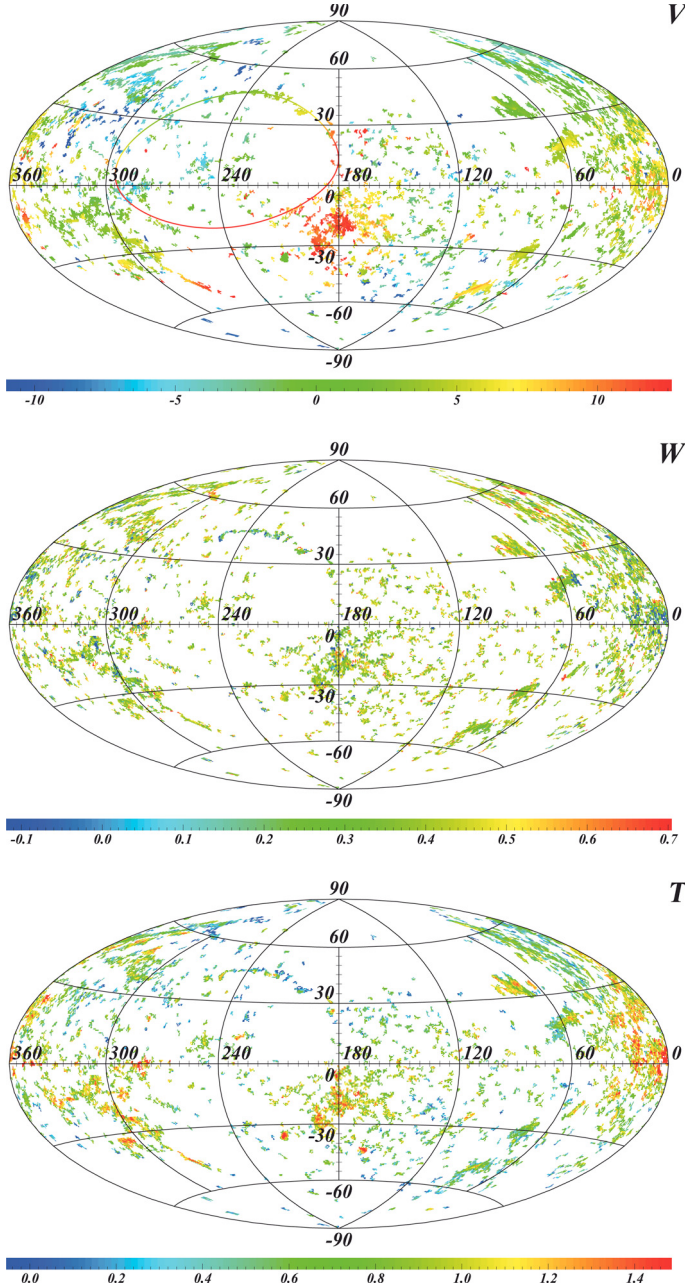


**Fig. 1.** The velocities, line-widths, and brightness temperatures in clouds of at least 7 GCs, compiled by our clustering algorithm. Shown are the objects for which the mean GC height is  $\geq 1.0$  K,  $FWHM \leq 3.0$   $\text{km s}^{-1}$ ,  $|V| \leq 15$   $\text{km s}^{-1}$  and the parameters of at least half of the GCs satisfy Eq. (4) of Paper II (components are likely not radio interferences). The color scales are for  $V$ ,  $\lg W$  and  $\lg T$ , respectively. The color line in the upper panel represents the sky positions and the velocities of our model ring (see Sect. 3.2).

clouds by applying the requirement  $|V| \leq 15 \text{ km s}^{-1}$  on the mean velocities of the clouds. In this way, we rejected 44 more small clouds. All remaining clouds are presented in Fig. 1.

When applying the described selection criteria on clusters, obtained with different values of the cutting level,  $S_{Cu}$ , of the dendrogram, we found that for  $0 < S_{Cu} < 0.27$  the number of GCs in the selected clouds increases rapidly. For  $0.27 \geq S_{Cu} < 0.75$ , the pictures similar to Fig. 1 remain nearly unchanged with only a slight maximum in the number of GCs for  $S_{Cu} = 0.44$ . After  $S_{Cu} = 0.75$ , the number of GCs starts to decrease, because

gradually wider and wider GCs are linked to the existing clouds and the average line widths of clouds grow above our selection limit. For Fig. 1, we chose the value of  $S_{Cu}$ , which gave the highest number of GCs in the selected clouds.

#### 4. Verschuur's clouds

From Fig. 1, we can see that the cold clouds around  $(l = 225^\circ, b = +44^\circ)$ ,  $(l = 236^\circ, b = +45^\circ)$ , and  $(l = 213^\circ, b = +41^\circ)$ , mentioned at the beginning of the previous section, are clearly visible. Moreover, in this figure these clouds seem to be part of a more extended narrow string of clouds, covering the sky about  $80^\circ$  from  $(l \approx 181^\circ, b \approx +20^\circ)$  to  $(l \approx 258^\circ, b \approx +47^\circ)$ . This is in good agreement with the remark by Heils & Troland (2003) that other narrow H I 21-cm emission lines can be found in the extended region around the clouds, studied in their paper. Nevertheless, they limited their interest to the longitude interval of  $200^\circ \leq l \leq 240^\circ$  and report the broken ribbon of cold H I gas stretching over  $20^\circ$  across the constellation Leo.

These clouds are plotted in Fig. 2 in more details. To better separate them from other features in the same sky region, we have used even more severe selection criteria here ( $FWHM \leq 2.7 \text{ km s}^{-1}$ ,  $2.25 \leq V \leq 11.55 \text{ km s}^{-1}$ ), compared to those for Fig. 1. However, because the noise GCs are effectively removed from the data also by using only clouds of 7 or more GCs, we dropped the requirement  $T \geq 1.0$  K to increase the sensitivity. The selection criteria, used for Fig. 1, led to the dendrogram cutting level  $S_{Cu} = 0.44$ . Now we changed the criteria and the considerations, described above, give somewhat higher value  $S_{Cu} = 0.53$ . As a result, we obtained a chain of clouds, which seems to follow some arc and which is well populated in its higher galactic longitude half and more opened at lower longitudes.

We can see a clear velocity gradient along this ribbon of clouds with the average velocities of the clouds increasing by about  $9 \text{ km s}^{-1}$  per arc length. A similar, but a much weaker gradient also holds for the line widths: the average  $FWHM$  of the clouds increases by  $1 \text{ km s}^{-1}$  from the higher galactic longitudes towards the lower longitudes. It also appears that the clouds tend to be brighter near their centers than in outer regions, which is expected behavior for real gas clouds. In this way, while the lower longitude part of the string of clouds is also interrupted in some places by voids, the coherence of its characteristics strongly indicates that it is really the same physical feature. It remains questionable whether the clouds at  $(l = 237^\circ, b = 24^\circ, V = 2.3 \text{ km s}^{-1})$  and  $(l = 184^\circ, b = 25^\circ, V = 4.5 \text{ km s}^{-1})$  also belong to the same structure because they deviate from the others considerably on the sky or in velocity. Therefore, we did not use them in the following discussion.

The observed structure is so smooth that it seemed interesting to try to model it. Since arced shapes often hint at circular structures, when seen under some angle to their plane, we decided to model this string of clouds and their velocities as a partial gas ring somewhere in space, which may move relative the local standard of rest (LSR) as a whole and also rotate around its center and expand away from this center. We found that such a model describes both the apparent location of the clouds on the sky and their observed velocities very well. According to this model, the center of the ring is located in the direction  $(l = 236.2^\circ \pm 0.9^\circ, b = -13.2^\circ \pm 0.3^\circ)$ , its apparent major axis is inclined by  $4.7^\circ \pm 0.9^\circ$  to the galactic plane, and the angle between the ring plane and the line of sight to its center is  $14.5^\circ \pm 0.3^\circ$ . The radius of the ring is seen under the angle of  $41.8^\circ \pm 0.3^\circ$  along the apparent major axis of the observed structure. The ring as a

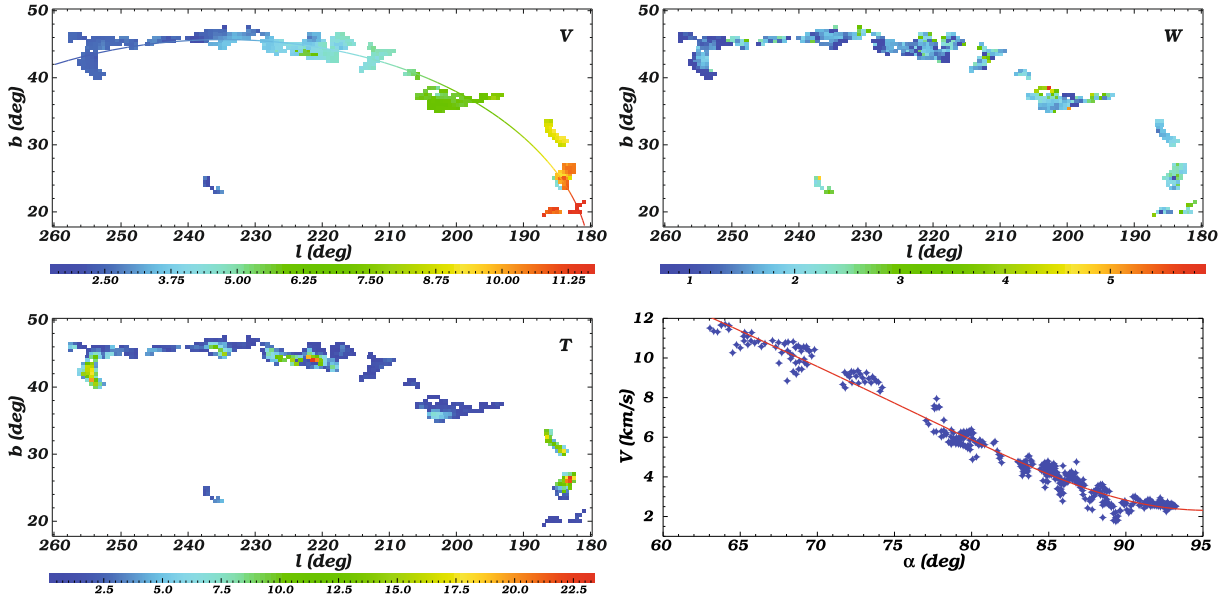


**Fig. 2.** The velocities, line-widths, and brightness temperatures of the clouds in the region of the observable part of the ring. Shown are the objects, represented by at least 7 GCs, for which the mean GC width  $FWHM \leq 2.7 \text{ km s}^{-1}$ ,  $2.25 \leq V \leq 11.55 \text{ km s}^{-1}$ , and the parameters of at least half of the GCs satisfy Eq. (4) of Paper II (components are likely not radio interferences). The color scales are for linear values of  $V$ ,  $W$ , and  $T$ . The color line in the *upper left panel* represents the sky positions and the velocities of our model ring. A more detailed comparison of the observed LSR velocities of the ring clouds (blue diamonds) with the model velocities (red line) is given in the *lower right panel* of the figure. Here the abscissa is a polar angle of the ring point in the ring plane.

whole moves with the velocity of  $21.0 \pm 0.5 \text{ km s}^{-1}$  in the direction ( $l = 193.3 \pm 1.2^\circ$ ,  $b = 2.2 \pm 0.7^\circ$ ) and rotates clockwise with the velocity of  $10.6 \pm 0.4 \text{ km s}^{-1}$ , and its expansion speed is  $26.2 \pm 0.7 \text{ km s}^{-1}$ . As errors in these parameters are given the 99.73% confidence limits obtained from the bootstrapping.

The projection of the model ring onto the sky is shown with a line in the first ( $V$ ) panels of Figs. 1 and 2. The color of the line corresponds to the line-of-sight velocity of each ring point. The fit of the model to the observed gas velocities is shown in the lower right part of Fig. 2. From Fig. 1, we can see that actually the same structure seems to continue even beyond the lower latitude border of Fig. 2, and it can be followed down to about ( $l = 225^\circ$ ,  $b = -19^\circ$ ). However, this continuation of the ring is rather sparsely populated with relatively small clouds and is located near the galactic plane, where the Gaussian decomposition cannot be considered to be reliable. Therefore, we do not discuss this continuation in more detail than just mentioning that, when the parameters of the ring were estimated only from a  $30^\circ$  segment of the whole ring (as seen from the ring center and indicated in the lower right panel of Fig. 2), in total the visible part of the ring may extend to nearly half ( $162^\circ$ ) of the full circle. For the other half there seems to be no good candidates for the same structure. But, of course, the location of the model ring is also uncertain in these regions.

## 5. The ring in space

In most HI profiles, the emission, corresponding to the clouds under discussion, appears as a very narrow and relatively strong line, not seriously blended by a broader-velocity, lower-intensity emission component. Therefore, it may seem to be easy to derive some estimates for the physical conditions inside these clouds from the parameters of our GCs. Unfortunately, as briefly mentioned in the Introduction, this is not true. Already, Verschuur & Knapp (1971) demonstrated that the shapes of these narrow emission lines are actually not Gaussian, but they are

considerably influenced by saturation. They derived the spin temperature by assuming the optical depth to be a Gaussian function of the frequency and fitting the observational data to the equation of transfer. We cannot even use this path, since the velocity resolution of the LAB data is more than 10 times lower than that of the data used by Verschuur & Knapp (1971), leaving the actual line-shapes mostly unresolved.

Nevertheless, we decided to take a further step by obtaining at least some preliminary estimate for the distance of the ring. In doing so, we followed the procedure described by Haud (1990). These estimates are based on the assumption that a correlation exists in cold HI clouds between the cloud's internal velocity dispersion and its linear dimensions, similar to the one observed for molecular clouds (Larson 1981 and many others since then). We do not discuss all these questions here, related to the existence or meaning of such correlation, but use it just as a possible tool, which may or may not give some acceptable results. We followed the same procedure exactly as described in Haud (1990) with the only exception that we did not correct the LSR velocities of the clouds to the galactic standard of rest (GSR), as it is most likely unjustified in this case. Instead, we removed the large-scale velocity gradients and projection effects in the ribbon clouds using our ring model. In this way, we obtained the distance estimates for all ring clouds and, with our model of the ring, converted them to estimates of the distance of the ring center.

As expected, we got fairly scattered results, but in general, the distance estimates of individual clouds agreed with our ring model, which indicates that the lower longitude tip of the band of clouds is located about twice as far from us as the higher longitude tip. As the scatter of the obtained estimates was considerably higher for estimates, based on smaller (covering fewer gridpoints of LDS observations) clouds than for those based on larger clouds, we decided to accept the weighted average of all determinations for the distance of the ring center and to use as weights the number of GCs in each cloud. In this way, we

obtained a distance estimate of  $126 \pm 82$  pc. The error estimate corresponds only to the scatter of individual distance estimates and does not account for uncertainties in the ring model or in the method, used for obtaining these distances. To this distance corresponds the linear radius of the model ring of 113 pc and the distance of the Verschuur's cloud A of 34 pc, which is in good agreement with the upper distance limit (45 pc) for this cloud, as established by Meyer et al. (2006).

Of course, a number of questions remain with such a model. First of all, why model this structure as a planar ring of gas clouds, when most processes, which may give the expansion velocities, obtained for this ring more likely have spherical symmetry? Moreover, when the ribbon of gas clouds covers nearly  $80^\circ$  in the galactic longitude, this corresponds in our model only to  $30^\circ$  along model ring itself. This means that we do not actually know anything about most of the ring, therefore its parameters may contain large systematic errors. Also, the distance estimates are based on rather arbitrary assumptions, and they are quite uncertain. Because the GCs most likely overestimate the widths of the actual underlying H I lines, they must be considered as upper limits for the corresponding actual distances.

Nevertheless, even such a model demonstrates the coherence of the observed clouds well, because it seems to give some indication of possible continuation of the structure even beyond the region studied here, and it is interesting to see that the distance estimates of the individual clouds and the ring model generally agree with respect to the orientation of the gas band in 3-dimensional space. Moreover, we have seen that the observed behavior of the gas stream at lower longitudes may be understood in the framework of this model: in these regions the distance of the clouds from the Sun increases so they apparently become smaller. As we have selected only relatively large clouds from our clustering results (at least 7 GCs in each cloud), we may lose most of the apparently smaller ones from our view. Therefore, beyond about ( $l = 182^\circ, b = 20^\circ$ ) and the distance 64 pc, the stream becomes fragmentary, and we can only observe some seemingly small clouds, which actually may have relatively large linear dimensions and line widths. As here we can no longer see the really smallest and coldest clouds, this may explain the increase in the average observable line widths in this region. But why then does the stream terminate so abruptly at its other end? This happens practically at the nearest point of the ring to the Sun.

Wolleben (2007) has proposed a model for the north polar spur (NPS) region. This model explains the results of the Dominion Radio Astrophysical Observatory Low-Resolution Polarization Survey (Wolleben et al. 2006), and the model consists of two synchrotron-emitting shells, S1 and S2. The same model shell S1 was used by Frisch (2009) to explain the direction of the interstellar magnetic field at the heliosphere, the polarization of light from nearby stars, and the kinematics of nearby clouds. We studied the mutual placement of these shells and our ring, and found that the ring intersects with the shell S2 in the direction ( $l = 256^\circ, b = 43^\circ$ ) at the distance of 33 pc from the Sun. This position matches the beginning of our band of clouds exactly, and the result is nearly independent of the fairly indefinite determination of the linear size of the ring. Farther to the higher longitudes, the ring continues inside the S2, and the ring clouds are probably destroyed by the shell. The ring leaves the shell at ( $l = 295^\circ, b = 4^\circ$ ) at the distance of 85 pc from the Sun. As with the lower longitude end of the gas stream, we may expect that the ring clouds, even if they exist there, are mostly unobservable at these distances.

A problem with this explanation of the observability of the ring clouds is that the ring intersects the S1 shell at ( $l = 235^\circ, b = 46^\circ, d = 33$  pc), but is still observable on both sides of this point. Maybe only a slight disturbance of the velocities of the ring clouds can be seen in this region. However, the explanation of the different behaviors of the ring clouds at the intersections with two different shells may lie in the different ages of these shells. According to Wolleben (2007), the S1 shell is about 6 million years old and only observable as a small part of “New-Loop” in the southern galactic hemisphere. The S2 shell is 1–2 million years old and seems to be much more active since it is responsible for the well known NPS. Therefore, we may expect that the S1 shell is no longer energetic enough to destroy the ring clouds, as they are destroyed by S2. By arbitrarily using the standard model for the kinematic age of stellar wind bubbles (Weaver et al. 1977), we may estimate that the age of the ring itself is about 2.5 million years, comparable to the age of the S2 shell. However, the physical mechanisms responsible for producing such cold clouds in the environment of the hot LB are still poorly understood (Stanimirović 2009).

## 6. Conclusions

So far we have decomposed the LAB database of H I 21-cm line profiles into the GCs (Paper I) and studied the statistical distributions of the obtained components (Papers II–IV). These distributions have revealed several interesting structures, but have given only the probabilities with which some particular GC may belong to one or another structure. In this Paper (V), we have proposed an algorithm for grouping similar GCs. In this way, we free ourselves from the need to study each GC separately, and we may expect that all the GCs of the “cloud” of similar components have the same nature. It may also be possible to obtain some additional physical information from the shapes and sizes of such clouds.

As a test problem, we considered the separation of clouds of the narrowest GCs as based on the preliminary considerations, this may be the hardest problem for our algorithm. We demonstrated that the algorithm easily found the coldest known H I clouds discovered decades ago by Verschuur (1969). As expected, the tests indicate that, depending on the cutting level of the clustering dendrogram, our approach may divide some larger clouds into separate, more coherent substructures, but it hopefully avoids the merging of unrelated features. This behavior was intentional, as it seems more appropriate to study a larger number of clouds where each represents a certain type of line features than to have fewer clouds that may mix GCs of different natures into one.

We also found that Verschuur's clouds form only a small part of a much longer ribbon of presumably very cold clouds covering the sky about  $80^\circ$ . As the gas velocities and line widths vary along this ribbon, we decided to model the whole structure as a part of a planar gas ring that may move in space as a whole and also rotate around and expand away from its center. Such a model represented the observed properties of the gas stream very well and indicated that the ring center must be located at a distance of  $126 \pm 82$  pc from the Sun in the direction ( $l = 236.2 \pm 0.9, b = -13.2 \pm 0.3$ ). The ring radius is about 113 pc, its apparent major axis is inclined by  $4.7 \pm 0.9$  to the galactic plane, and the angle between the ring plane and the line of sight to its center is  $14.5 \pm 0.3$ . The ring as a whole moves with a velocity of  $21.0 \pm 0.5 \text{ km s}^{-1}$  in the direction ( $l = 193.3 \pm 1.2, b = 2.2 \pm 0.7$ ), it rotates clockwise with the velocity of  $10.6 \pm 0.4 \text{ km s}^{-1}$ , and its expansion speed is

$26.2 \pm 0.7$  km s $^{-1}$ . In the framework of such a model, the apparent gradual weakening of the ring clouds at the lower longitude tip of the stream is explained by increasing distances between the Sun and the ring clouds in this region, and the abrupt end of the stream at the higher longitude part is caused by the intersection of the ring with the S2 supernova shell from the model by Wolleben (2007).

In many respects most of other clouds, seen in Fig. 1, are somewhat different from the ring clouds: lines are slightly wider, velocities less coherent over the structures etc. We did not attempt to model these features, but because the line widths of these clouds are also small, they must be relatively cold clouds, so not very large spatially. As these clouds of presumably small linear dimensions cover fairly large areas on the sky, they probably cannot be located very far from the Sun; therefore, the studies of such narrow-lined clouds may give useful information about the gas in the solar neighborhood. Usually this gas is studied through corresponding absorption lines, which allow estimation of physical conditions in the local gas. The HI 21-cm emission line is less useful in this respect, but may still be usable for large-scale surveys to find out possible interesting features in the local neighborhood.

As a result, we may state that the ring clouds seem to be a unique feature on the sky. Most likely they are the coldest clouds observable in the HI 21-cm emission line. Also, slightly warmer clouds (clouds with slightly wider 21-cm emission lines) may be related to local gas structures inside or near the LB. Some properties of these clouds may be similar to those with the HI self-absorption features, observed predominantly near the galactic plane, where our approach to the emission data is most likely not applicable, but in this paper we have not studied this in enough detail to make firm statements.

**Acknowledgements.** The author would like to thank W. B. Burton for providing the preliminary data from the LDS for program testing prior to the publication of the survey. A considerable part of the work on creating the decomposition program was done during the stay of U. Haud at the Radioastronomical Institute of Bonn University (now Argelander-Institut für Astronomie). The hospitality of the Institute staff members is highly appreciated. We thank Drs. I. Kolka, E. Saar, P. Tenjes, and K. Annuk for fruitful discussions. We also thank our anonymous referee, whose suggestions improved the clarity of the paper. The project was supported by the Estonian Science Foundation grant no. 7765.

## References

- Bajaja, E., Arnal, E. M., Larrarte, J. J., et al. 2005, A&A, 440, 767
- Blitz, L. 1993, Giant Molecular Clouds. In Protostars and Planets III, ed. E. H. Levy, & J. I. Lunine (Tucson & London: The Univ. Arizona), 125
- Blitz, L., & Stark, A. A. 1986, ApJ, 300, 89
- Carr, J. S. 1987, A&A, 323, 170
- de Heij, V., Braun, R., & Burton, W. B. 2002, A&A, 391, 159
- Dickey, J. M., McClure-Griffiths, N. M., Gaensler, B. M., et al. 2003, ApJ, 585, 801
- Dobashi, K., Bernard, J. P., & Fukui, Y. 1996, ApJ, 466, 282
- Frisch, P. C. 2009, Space Sci. Rev., 143, 191
- Gibson, S. J., Taylor, A. R., Higgs, L. A., et al. 2000, ApJ, 540, 851
- Hartmann, L. 1994, The Leiden/Dwingeloo Survey of Galactic Neutral Hydrogen, Ph.D. Thesis, Leiden Univ.
- Haud, U. 1990, A&A, 230, 145
- Haud, U. 2000, A&A, 364, 83 (Paper I)
- Haud, U. 2008, A&A, 483, 469 (Paper IV)
- Haud, U., & Kalberla, P. M. W. 2006, Balt. Astron., 15, 413 (Paper II)
- Haud, U., & Kalberla, P. M. W. 2007, A&A, 466, 555 (Paper III)
- Heils, C., & Troland, T. H. 2003, ApJ, 586, 1067
- Hosokawa, T., & Inutsuka, S.-I. 2007, ApJ, 664, 363
- Kalberla, P. M. W., & Haud, U. 2006, A&A, 455, 481
- Kalberla, P. M. W., Burton, W. B., Hartmann, D., et al. 2005, A&A, 440, 775
- Kavars, D. W., Dickey, J. M., McClure-Griffiths, N. M., Gaensler, B. M., & Green, A. J. 2005, ApJ, 626, 887
- Knapp, G. R., & Verschuur, G. L. 1972, AJ, 77, 717
- Kramer, C., Stutzki, J., Rhring, R., et al. 1998, A&A, 329, 249
- Lada, E. A., Bally, J., & Stark, A. A. 1991, ApJ, 368, 432
- Larson, R. B. 1981, MNRAS, 194, 809
- Larson, R. B. 2003, Rep. Prog. Phys., 66, 1651
- Loren, R. B. 1989, ApJ, 338, 902
- Meyer, D. M., Lauroesch, J. T., Heils, C., Peek, J. E. G., et al. 2006, ApJ, 650, 67
- Nidever, D. L., Majewski, S. R., & Burton, W. B. 2008, ApJ, 679, 432
- Nozawa, S., Mizuno, A., Teshima, Y., et al. 1991, ApJS, 77, 647
- Redfield, S., & Linsky, J. L. 2008, ApJ, 673, 283
- Stanimirović, S. 2009, Space Sci. Rev., 143, 291
- Stutzki, J., & Güsten, R. 1990, ApJ, 356, 513
- Thilker, D. A., Braun, R., & Walterbos, R. A. M. 1998, A&A, 332, 429
- Verschuur, G. L. 1969, ApL, 4, 85
- Verschuur, G. L., & Knapp, G. R. 1971, AJ, 76, 403
- Weaver, R., McCray, J., Castor, J., Shapiro, P., & Moore, R. 1977, ApJ, 218, 377
- Williams, J. P., de Geus, E. J., & Blitz, L. 1994, ApJ, 428, 693
- Wolleben, M. 2007, ApJ, 664, 349
- Wolleben, M., Landecker, T. L., Reich, W., et al. 2006, A&A, 448, 411